

Active learning of linear interatomic potentials

Evgeny V. Podryabinkin, Alexander V. Shapeev

December 9, 2024

Abstract

This paper introduces an active learning approach to the fitting of machine learning interatomic potentials. Our approach is based on the D-optimality criterion for selecting atomic configurations on which the potential is fitted. It is shown that the potentials fitted with this approach have improved transferability. Moreover, the proposed active learning approach is highly efficient in training potentials on the fly, ensuring that no extrapolation is attempted.

Keywords: Interatomic potential, Active learning, Learning on the fly, Machine learning, Molecular dynamics, Moment Tensor Potential

1 Introduction

In molecular dynamics (MD), as a rule, one of the following two classes of interatomic interaction models is used. The first class is the empirical interatomic potentials [19, 39]—they are very computationally efficient and allow for simulating large atomistic systems for microseconds of simulation time. However, they typically yield only qualitative accuracy. The other class is quantum-mechanical (QM) models, such as the density functional theory (DFT) [15]. They are very accurate, but computationally expensive. Their applicability is typically limited to hundreds of atoms and hundreds of picoseconds of simulation time.

Several directions of developing the models that would be both accurate and computationally efficient have been pursued. They include the so-called linear scaling DFT [1, 34, 14] that ensures that the algorithmic complexity grows linearly when the size of the atomistic system increases beyond hundreds of atoms. Another direction is the development of semi-empirical models, such as the tight-binding model [19], whose accuracy and efficiency is between those of the empirical potentials and DFT. In this paper we pursue a more recent approach based on machine learning.

Application of machine learning (ML) has recently been put forward as a promising idea that would combine the accuracy of the QM models and the efficiency of the interatomic potentials [2, 3, 5, 7, 8, 9, 10, 17, 21, 27, 29, 32, 37, 38]. Such machine-learning interatomic potentials (MLIPs) postulate a partitioning of the interatomic interaction energy into individual contributions of the atoms (and sometimes bonds, bond angles, etc.) and assume a certain functional form for such a contribution, making it a function of the positions of

the neighboring atoms, typically with hundreds or more parameters. These parameters are found by requiring the energy, forces and/or stresses predicted by a MLIP to be close to those obtained by a QM model on some atomic configurations. These configurations are called the *training set*, and finding the parameters of a MLIP is known as *training* or *fitting*. One of the important features of MLIPs are their ability to approximate potential energy surfaces with arbitrary accuracy (at least theoretically) by increasing the number of parameters and the training set. It should be noted that there are other ML-based atomistic models of solids, including those predicting the energy directly without partitioning it [18, 30], or constructing a density functional in a DFT with machine learning [36]. A recent overview of ML-based models of materials can be found in [28].

Each of the existing MLIPs has a nontrivial functional form accounting exactly for the physical symmetries of interatomic interaction. Namely, a MLIP should be invariant with respect to translation, rotation, and reflection of the space, and also permutation of chemically equivalent atoms. In addition, the potential should have a local support (i.e., depend on surrounding atoms only within a finite cut-off radius) and be smooth with respect to atoms coming and leaving the support. In many instances, it is achieved by designing a fixed number of descriptors [4, 6]—scalar functions satisfying all the symmetries and uniquely encoding each atomic environment, and assuming that a MLIP is an arbitrary function (which we call the *regression model*) of these descriptors. This idea was first put forward by Parinello and Behler [9] proposing an ML model, which they called a neural network potential (NNP), based on their descriptors and neural networks as the regression model. Since then, there has been many works on NNPs, see the review papers [7, 8] and references therein, and also more recent works [2, 17, 21, 27, 29, 35]. Another group of authors adopted the Gaussian process regression framework [5]. They used the coefficients of spherical harmonics expansion of the smeared atomic positions as descriptors and used the kernel-based ML model, where the kernel was based on the distance between the vectors comprised of those coefficients. In a follow-up paper, [37], the authors refined this idea by proposing the smooth overlap of atomic positions kernel, bypassing the step of designing the descriptors. For other examples of using Gaussian process regression for constructing interatomic potentials refer to [3, 16]. Two closely related works, [13, 26], use Gaussian process regression to predict the forces on atoms directly, without predicting the energy and taking its gradient. Finally, [38] proposes a linear regression model with spherical harmonics coefficients as the basis functions. In the present work, we use the moment tensor potentials (MTP) [32]. These potentials adopt a linear regression model with polynomial-like functions of atomic coordinates as the basis functions. The MTPs can be interpreted as having descriptors which are based on tensors of inertia of atomic environments.

All the MLIPs described above, with the exception of [38], allow for improving their accuracy through increasing the number of the fitting parameters. However, the approximation properties of ML potentials depend not only on their algebraic form, but also on the training set used to fit them. Choosing a good training set for a potential with many parameters (say, more than ten) proves to be a highly nontrivial practical problem. Indeed, all the existing MLIPs are interpolative, they fail to give reasonable answers outside their training domain. Therefore, a good training set should make a MLIP to be interpolative

over all the relevant configurations. Obviously, the more parameters a MLIP involves, the larger and more diverse the training set is required in order to fit such a MLIP.

The problem of choosing a proper training set for the fitting of a reliable MLIP is connected to the problem of transferability—the ability of interatomic potentials to extrapolate, i.e., give reasonable predictions outside the training domain (e.g., predict the double vacancy formation energy if only single vacancies are present in the training set). It is hardly expected that a MLIP can extrapolate beyond the training domain, but even developing a reliable problem-specific MLIP that would accurately interpolate within the training domain is non-trivial, as pointed out, for instance, by Behler [8, Section 4]. As an illustration of this, the authors of [37] sampled gamma surfaces and included them in the training set, which allowed them to compute the properties of dislocations accurately with the exception of their Peierls barrier. To accurately reproduce the latter they devised a more complicated scheme of generating configurations from the MD trajectories using one version of their potential in order to fit a better version of their potential.

An attractive idea is to attempt to sample the entire space of atomic environments within, for example, a constraint on the minimal interatomic distance. It is, however, not clear how to do this with sufficient accuracy due to extremely high dimensionality of the space of atomic neighborhoods. Therefore, in practice, the training set is usually generated by specially designed sampling procedures such as, for example, random perturbations of ideal crystalline configurations [38], or sampling from an AIMD or a classical MD with another interatomic potential [37]. These sampling procedures, however, do not ensure that the training set covers fully, without “gaps”, the region in the configuration space required for training MLIPs reliably. In other words, a potential resulted from such a training procedure may later encounter configurations on which this potential will have to extrapolate.

The problem of extrapolation could be resolved if a MLIP were able to detect extrapolative configurations, obtain the QM data for those configurations, and be re-trained. In this scenario, known as learning on the fly, the extrapolation problem (or the transferability problem) would be solved by reliably predicting whether a potential is extrapolating on a given configuration. Alternatively, in the case when computing the QM data cannot be done on the fly, the selection of extrapolative configurations can be done offline together with the training set sampling, thus improving the transferability of the fitted potential.

Both scenarios are related to a set of ML techniques called active learning (AL). In contrast to passive learning in which a potential learns every configuration in the training set, in AL a potential is trained only on a set of selected configurations. The key component of any AL method is, thus, its *query strategy*—an algorithmic criterion for deciding whether a given configuration can be treated reliably by an ML model, or we need to re-train our model by querying the QM data for this configuration. If such decision can be made reliably then, as we show in this paper, we do not have to ensure that the training set generated offline has all the representative configurations.

A general overview of AL approaches can be found in [31]. In the context of interatomic potentials, the first work that proposed AL was [20] putting forward a Bayesian query-by-committee strategy. AL was applied by Behler to the neural network potentials [8, Section 4], using the query by committee-type AL strategy. Finally, the authors of [12, 11] train a

machine learning model predicting the force errors based on the distance between a given atomic configuration and the training set. A very natural AL approach, which has not yet been implemented in practice, would be to use the Bayesian predictive variance, shown to correlate with the actual error, e.g., in [36]. We note that there are other, non-AL types of learning on the fly, that take into account also the QM data once in several MD time steps [26].

In this paper we propose another AL approach for MLIPs based on the D-optimality criterion [31, Section 3.5] allowing for detecting the configurations on which a MLIP extrapolates. We apply our AL approach to the fitting of MTPs, however, it is easily generalizable to a any other linear potential, i.e., a potential whose energy depends linearly on the parameters, such as SNAP or GAP. In principle, we can apply AL to atomistic systems with any number of chemically different types of atoms, however, the linear potentials developed to date are only applicable to systems with a single type of atoms. We demonstrate that our AL approach allows one to train potentials on the fly with a limited number of QM calculations (occurring, typically, within the first few picoseconds of the MD simulation time) without loss in accuracy. In addition, we show that even without learning on the fly, AL can “optimize” the training set, in the sense of extracting a significantly smaller subset, training on which reduces the maximal error and improves transferability.

The structure of the paper is as follows. In Section 2 we introduce the interatomic potentials in general, the MTPs in particular, and discuss their fitting. In Section 3 we detail our AL approach and present its three variants. In Section 4 we numerically compare the proposed AL approach with passive learning, and demonstrate its accuracy and efficiency in the learning-on-the-fly scenario. We discuss the results in Section 5 and give concluding remarks in Section 6.

2 Machine Learning Interatomic Potentials

2.1 Basic definitions

Consider an atomistic system with N atoms described by the collection of their positions

$$x = (x_1, \dots, x_N) = (x_i)_{1 \leq i \leq N},$$

each position is a three-dimensional vector, $r_i \in \mathbb{R}^3$. All the atoms are assumed to be chemically equivalent. We assume periodic boundary conditions with the supercell

$$L = (l_1 \ l_2 \ l_3) \in \mathbb{R}^{3 \times 3},$$

given by the linearly independent vectors $l_i \in \mathbb{R}^3$. This means that each x_i is repeated periodically as $x_i + sL$ for all $s \in \mathbb{Z}^3$. We call the atomic positions x , together with the respective L , the atomistic *configuration*.

Suppose we can compute, for a given configuration x , the QM energy $E^q(x)$, forces $(f_i^q(x))_{1 \leq i \leq N}$ and stresses $\sigma^q(x)$. Such computation typically involves resolving the electronic structure and is very expensive. For the purpose of our paper, we treat such computation as a black box.

2.2 Moment Tensor Potential

We next assume that each atom interacts with its neighborhood defined by a cut-off distance $R_{\text{cut}} > 0$. The neighborhood of atom i , $1 \leq i \leq N$, is defined as a collection (tuple) of vectors pointing from atom i to all the atoms and their periodic extensions, excluding the atom itself, that are not farther than R_{cut} :

$$\mathbf{r}_i := (x_j + sL - x_i)_{1 \leq j \leq N, s \in \mathbb{Z}^3, 0 < |x_j + sL - x_i| \leq R_{\text{cut}}}.$$

The exact ordering of the elements of \mathbf{r}_i is not important, as all the functions of \mathbf{r}_i that we will consider are permutation invariant.

We assume that the total interaction energy of this configuration is

$$E(x) = \sum_{i=1}^N V(\mathbf{r}_i), \quad (1)$$

where V is the interatomic potential—a scalar function of the neighborhood $\mathbf{r}_i = (r_{i,1}, \dots, r_{i,n})$, where the number of atoms in the neighborhood, n , may depend on i .

We use the Moment Tensor Potentials (MTPs) [32]

$$V(\mathbf{r}_i) = \sum_{j=1}^m c_j B_{\alpha_j}(\mathbf{r}_i),$$

where the basis functions B_{α_j} are indexed by $k \times k$ integer symmetric matrices $\alpha_j \in \mathbb{N}^{k \times k}$ (where $\mathbb{N} = \{0, 1, \dots\}$) as follows. We let $\mathcal{N} := \{1, \dots, N\}$ and define

$$B_{\alpha}(\mathbf{r}_i) = \sum_{\gamma \in \mathcal{N}^k} \left(\prod_{\substack{\ell, m=1 \\ m < \ell}}^k (r_{i, \gamma_m} \cdot r_{i, \gamma_\ell})^{\alpha_{m, \ell}} \right) \left(\prod_{\ell} f_{\alpha_{\ell, \ell}}(|r_{i, \gamma_\ell}|) \right),$$

where $f_{\mu} = f_{\mu}(\rho)$ ($\mu \in \mathbb{N}$) is the set of radial basis functions that vanish for $\rho > R_{\text{cut}}$, and R_{cut} is the cut-off radius of the potential. We refer the reader to [32] for more details on MTPs.

According to (1), the energy of the configuration x can be computed as

$$E(x) = \sum_{i=1}^N \sum_{j=1}^m c_j B_{\alpha_j}(\mathbf{r}_i).$$

We define $b_j(x) := \sum_{i=1}^N B_{\alpha_j}(\mathbf{r}_i)$ and thus write

$$E(x) = \sum_{j=1}^m c_j b_j(x).$$

In addition to fitting to the energy, one also fits to forces acting on atoms

$$f_j(x) = -\nabla_{x_j} E(x), \quad 1 \leq j \leq N \quad (2)$$

and the stress tensor

$$\sigma(x) = (\nabla_L E(x)) L^{\top}. \quad (3)$$

Forces and stresses of x involve gradients of b_j . From the definition it seems that computing B_{α} is very expensive, however, there is a fast algorithm for computing B_{α} and their derivatives [32].

2.3 Fitting (training)

An MTP is uniquely determined by the values of α_j (which are assumed to be fixed throughout) defining the algebraic form of the interatomic potential, and the values of the fitting parameters c_j . The latter are found through fitting to the QM energy, forces, and stresses on a set of configurations $X_{\text{TS}} = \{x^{(1)}, \dots, x^{(K)}\}$ which we call the *training set*.

The simplest form of fitting is requiring $E(x^{(k)}) = E^{\text{q}}(x^{(k)})$. Expanding the left-hand side yields system of linear algebraic equations (SLAEs) on the coefficients c_j :

$$\sum_{j=1}^m c_j b_j(x^{(k)}) = E^{\text{q}}(x^{(k)}). \quad (4)$$

In the matrix notation, we can write this system as $\mathbf{B}c = R$,

$$\mathbf{B} = \begin{pmatrix} b_1(x^{(1)}) & \dots & b_m(x^{(1)}) \\ \vdots & \ddots & \vdots \\ b_1(x^{(K)}) & \dots & b_m(x^{(K)}) \end{pmatrix}.$$

This system is typically overdetermined ($K \geq m$), therefore we define the solution through the pseudoinverse by $c := (\mathbf{B}^{\top}\mathbf{B})^{-1}\mathbf{B}^{\top}R$.

If the configurations in the training set X_{TS} are also provided with the forces $f^{\text{q}}(x^{(k)})$ and stresses $\sigma^{\text{q}}(x^{(k)})$ one can add two more families of equations in addition to fitting to the energy:

$$C_{\text{f}}f_{\ell}(x^{(k)}) = C_{\text{f}}f_{\ell}^{\text{q}}(x^{(k)}), \quad C_{\text{s}}\sigma(x^{(k)}) = C_{\text{s}}\sigma^{\text{q}}(x^{(k)}). \quad (5)$$

These equations are combined into a single least-square minimization problem, therefore we need to introduce the coefficients C_{f} and C_{s} determining the relative importance of the force- and stress-fitting equations relative to the energy-fitting equation. Expanding the left-hand side of (5) yields the following equations:

$$C_{\text{f}} \sum_{j=1}^m c_j \nabla_{x_{\ell}} b_j(x^{(k)}) = -C_{\text{f}} f_{\ell}^{\text{q}}(x^{(k)}), \quad \ell = 1, \dots, N^{(k)}, \quad 1 \leq k \leq K, \quad (6)$$

$$C_{\text{s}} \sum_{j=1}^m c_j (\nabla_L b_j(x^{(k)})) L^{\top} = C_{\text{s}} \sigma^{\text{q}}(x^{(k)}), \quad 1 \leq k \leq K. \quad (7)$$

3 Active Learning

In the AL framework we are given a large set of unlabeled dataset, X_{US} (i.e., configurations x with no given $E^{\text{q}}(x)$, $f^{\text{q}}(x)$, $\sigma^{\text{q}}(x)$), and we need to extract a smaller subset, X_{TS} , for which we then compute the QM data and use it for the fitting of a MLIP. A particular way of selecting configurations for X_{TS} is called the *query strategy*. In our context, a query strategy is a criterion on whether a given configuration $x^* \in X_{\text{US}}$ should be added to X_{TS} , by possibly removing another configuration from X_{TS} .

An overview of various query strategies is presented in [31]. In the present work we employ the variance reduction query strategy based on the D-optimality criterion [31, Section 3.5].

A way to derive the D-optimality criterion is to assume that the right-hand side of the equations (4), (6), (7) has a Gaussian random noise and we want to select m out of K equations such that the noise in the solution is minimized. This is equivalent to choosing a subset of equations (4), (6), (7) such that its matrix $\mathbf{A} \in \mathbb{R}^{m \times m}$ has the maximal determinant by its absolute value. Those configurations $x^{(k)}$ that correspond to the selected equations hence form X_{TS} .

The active learning algorithm is determined by the following two choices: what equations are used for the fitting and what equations are used for the selection of the configurations. It should be noted that the two sets of equations need not coincide: for instance, the fitting can be done over all the equations (4), (6), (7), but the selection can be done only based on (4). In the present work we use all the equations for the fitting, and three different versions of the query strategy, as detailed below.

Query strategy QS₁: Selection by the energy-fitting equation

This query strategy, labeled as QS₁, involves only the energy-fitting equation (4). Let $x^* \in X_{\text{US}}$ and we need to decide whether to add it to $X_{\text{TS}} = \{x^{(1)}, \dots, x^{(m)}\}$. The rows of the matrix \mathbf{B} corresponding to $x^{(i)} \in X_{\text{TS}}$ are:

$$\mathbf{A} = \begin{pmatrix} b_1(x^{(1)}) & \dots & b_m(x^{(1)}) \\ \vdots & \ddots & \vdots \\ b_1(x^{(m)}) & \dots & b_m(x^{(m)}) \end{pmatrix}.$$

Following the maxvol algorithm [22], we form the row-vector

$$C := (b_1(x^*) \quad \dots \quad b_m(x^*)) \mathbf{A}^{-1}. \quad (8)$$

If we replace the k -th row of \mathbf{A} by $(b_1(x^*) \dots b_m(x^*))$ then $|\det \mathbf{A}|$ will change by a factor of $|C_k|$. The easiest way to see this is to use the Cramer's formula for, e.g., $k = 1$:

$$C_1 = \frac{\begin{vmatrix} b_1(x^*) & \dots & b_m(x^*) \\ b_1(x^{(2)}) & \dots & b_m(x^{(2)}) \\ \vdots & & \vdots \\ b_1(x^{(m)}) & \dots & b_m(x^{(m)}) \end{vmatrix}}{\begin{vmatrix} b_1(x^{(1)}) & \dots & b_m(x^{(1)}) \\ b_1(x^{(2)}) & \dots & b_m(x^{(2)}) \\ \vdots & & \vdots \\ b_1(x^{(m)}) & \dots & b_m(x^{(m)}) \end{vmatrix}}.$$

Our query strategy is thus as follows. If

$$\theta(x^*) := \max_{1 \leq k \leq m} |C_k| > 1 + \gamma, \quad (9)$$

where $\gamma \geq 0$, then we add x^* to the training set and remove $x^{(k)}$ with $k = \arg \max_k |C_k|$; otherwise, we keep the X_{TS} as is. This procedure guarantees that if x^* is added to X_{TS} then

$|\det \mathbf{A}|$ is increased by a factor of $1 + \gamma$. If in the algorithm one stores \mathbf{A}^{-1} instead of \mathbf{A} then the complexity of computing $\theta(x^*)$ is only $O(m^2)$. When \mathbf{A} changes, it also takes $O(m^2)$ operations to update \mathbf{A}^{-1} using the Sherman-Morrison [33] rank-one update.

It is worthwhile noting that the elements of C can be interpreted as the coefficients of expressing $E(x^*)$ through $E(x^{(k)})$:

$$E(x^*) = \sum_{k=1}^K C_k E(x^{(k)}).$$

Hence we can say that if all $|C_k| \leq 1$ then we are *interpolating* the predicted value of the energy, $E(x^*)$, through the energies $E(x^{(k)}) = E^q(x^{(k)})$. Hence, $\theta(x^*)$ defined by (9) has a meaning of a degree of extrapolation that we commit when evaluating $E(x^*)$. Hence we call $\theta(x^*)$ the *extrapolation grade* and the parameter $\gamma \geq 0$ defines the maximal allowed extrapolation grade. It should be emphasized that $\theta(x^*)$ does not depend on the QM data and is therefore a geometric feature of the configuration x^* .

Query strategy QS₂: Selection by all equations

In this query strategy, QS₂, the matrix \mathbf{A} is formed by m equations chosen from (4), (6), (7). Thus, each configuration x^* yields $1 + 3N + 6$ rows in place of (8),

$$\mathbf{C} = \underbrace{\begin{pmatrix} b_1(x^*) & \dots & b_m(x^*) \\ C_f \nabla_{x_1} b_1(x^*) & \dots & C_f \nabla_{x_1} b_m(x^*) \\ \vdots & \vdots & \vdots \end{pmatrix}}_{=: \mathbf{B}} \mathbf{A}^{-1},$$

and it is selected for training if

$$\max_{k,j} |C_{kj}| > 1 + \gamma. \quad (10)$$

We then use the maxvol algorithm [22] to maximize $|\det \mathbf{A}|$; it is a greedy algorithm replacing rows of \mathbf{A} with rows of \mathbf{B} until $\max_{k,j} |C_{kj}| \leq 1 + \gamma$. The algorithm is detailed in Appendix A. Note that in this query strategy there may be more than one row of \mathbf{A} corresponding to one configuration, and thus less than m configurations may be selected into the training set. The algorithm complexity is $O(Nm^2)$.

Query strategy QS₃: Selection by neighborhoods

To formulate the last approach we suppose, for the sake of argument, that we could also fit to the site energies,

$$V(\mathbf{r}_i^{(k)}) \equiv \sum_{j=1}^m c_j B_{\alpha_j}(\mathbf{r}_i^{(k)}) = V_i^q(x^{(k)}) \quad 1 \leq k \leq K, \quad 1 \leq i \leq N^{(k)}. \quad (11)$$

Thus, in the third approach, QS₃, **A** is formed by the equations (11). We proceed similarly to QS₂ and compose

$$\mathbf{C} = \underbrace{\begin{pmatrix} B_{\alpha_1}(\mathbf{r}_1^*) & \dots & B_{\alpha_m}(\mathbf{r}_1^*) \\ \vdots & \vdots & \vdots \\ B_{\alpha_1}(\mathbf{r}_N^*) & \dots & B_{\alpha_m}(\mathbf{r}_N^*) \end{pmatrix}}_{=: \mathbf{B}} \mathbf{A}^{-1}.$$

Then if $\max_{k,j} |C_{kj}| > 1 + \gamma$ then we replace the rows in **A** with the rows in **B** and update X_{TS} accordingly. As in QS₂, there may be more than one row of **B** corresponding to one configuration, and thus the training set may contain less than m configurations. The algorithm complexity is the same as that of QS₂, $O(Nm^2)$.

3.1 Applications of Active Learning

Learning on the fly

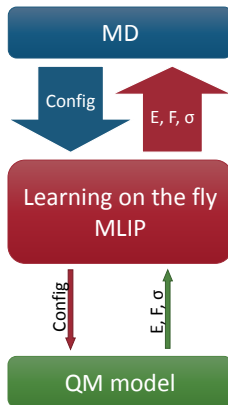


Figure 1: Workflow in actively learning a potential on the fly. The AL MLIP receives from MD a configuration x^* and occasionally decides to pass it to the QM model. Then it returns the predicted energy, forces, and stresses back to MD.

The AL methodology naturally translates into a learning on-the-fly scheme that combines the interatomic potential evaluation and its learning into a single routine, see Fig. 1. At each iteration of, for instance, an MD process, an unlabeled configuration x^* comes as an input to an AL procedure, that does the following.

1. Update X_{TS} (and hence **A**) with x^* if necessary.
2. If X_{TS} is updated then compute $E^q(x^*)$, $f^q(x^*)$, and $\sigma^q(x^*)$ and re-fit c_1, \dots, c_m .
3. Return $E(x^*)$, $f(x^*)$, $\sigma(x^*)$ according to the current values of c_1, \dots, c_m .

Note that in this scheme the parameter γ controls the efficiency of the learning-on-the-fly scheme, allowing to ignore configurations which increase $|\det \mathbf{A}|$ only slightly and perform expensive QM calculations only for sufficiently “new” configurations. In practice, there is

an optimal range of γ for which the QM calculations are not done too often, and on the other hand, the extrapolation does not significantly decrease the accuracy of the potential, see Section 4.2.

A posteriori error control

There may be a situation when computing extra QM data is not possible on the fly, however one wishes to have an assessment of the applicability of a MLIP to a given configuration x^* while running MD. This can be done by computing its extrapolation grade, $\theta(x^*) := \max_k |C_k|$. Note that the cost of evaluating $\theta(x^*)$ is as cheap as a matrix-vector multiplication (or a matrix-matrix multiplication for QS₂ and QS₃), as we do not need to consider the cost of evaluating $(b_1(x^*) \dots b_m(x^*))$ in (8) (and \mathbf{B} for QS₂ and QS₃) since it is required for computing $E(x)$ in any case. In the next section we will show that the error and $\theta(x^*)$ correlate.

Even more important than simply knowing θ for configurations appeared in MD, we can store the configurations with high θ in order to perform the QM calculations and refit MLIP on them later.

Optimization of the training set

We will show that applying the proposed AL methods to offline learning allow one to reduce the size of X_{TS} (resulting in acceleration of the training stage) while keeping the accuracy essentially at the same level as for the fitting on the entire evaluation set. Furthermore, we will show that, as compared to passive learning, the resulting interatomic potentials have better *transferability*—the ability of the potential to make a prediction for configurations sufficiently different from those in the training set. We argue that this is achieved because AL, in some sense, selects the “most different” configurations for training, resulting in a smaller degree of extrapolation if used on a different evaluation set.

4 Testing

In this section we test the proposed AL schemes. In Section 4.1 we test the accuracy of the AL potentials, showing that selecting and fitting on a smaller set of configurations does not, essentially, increase the error and at the same time improves transferability. Then, in Section 4.2, we will test learning on the fly.

All tests are performed in a cubic supercell of 128 Lithium atoms arranged in a BCC lattice. The length of the supercell in each direction is greater than twice the cutoff radius, $2R_{\text{cut}} = 10\text{\AA}$. This ensures that each atomic neighborhood does not contain multiple periodic images of a single atom.

The energies, forces, and stresses were computed using DFT with VASP [25, 23, 24]. Lithium is an alkaline metal with one valence electron and therefore its electronic structure can be computed faster than for the other elements, which is helpful in collecting large statistics for the tests.

Table 1: RMS fitting errors in energy, forces and stresses for MTPs with different number of basis functions, m . The root-mean-square (RMS) and the maximum errors are quoted.

m	Energy error		Force error		Stress error	
	(meV/atom)		(eV/Å)	(%)	(GPa)	(%)
10	0.35		0.023	7.4	0.073	7.0
30	0.22		0.018	5.8	0.060	5.8
100	0.19		0.016	5.1	0.052	5.2
300	0.17		0.015	4.9	0.045	4.4
1000	0.15		0.015	4.8	0.040	3.8

Table 2: Errors of fitting of different AL approaches.

Query strategy	# X_{TS}	energy error		force error		stress error	
		(meV/atom)		(eV/Å)		(GPa)	
		RMS	max	RMS	max	RMS	max
passive	24000	0.19	0.82	0.016	0.13	0.052	0.13
random	100	0.21	0.92	0.017	0.28	0.057	0.14
QS ₁	100	0.21	0.78	0.016	0.10	0.053	0.13
QS ₂	84	0.25	0.89	0.016	0.10	0.056	0.13
QS ₃	92	0.23	0.79	0.016	0.09	0.057	0.13

4.1 Accuracy of Active Learning

Accuracy convergence on MTP sequence

In the first test, the database was comprised of four AIMD trajectories sampling an NVT-ensemble at temperature $T = 300$ K, each trajectory ran for 6 000 time steps, each time step was 1 fs. A sequence of MTPs with different number of basis functions, m , was generated; the more basis functions are included, the better is the accuracy. The fitting errors are given in Table 1. Here and in what follows we report the root-mean-square (RMS) error and the maximum error. As can be seen, the potentials systematically converge, however, increasing the number of basis functions beyond 100, essentially, does not reduce the error. Therefore the results for the subsequent tests will be quoted for the same set of 100 basis functions.

Errors of fitting

Next, we compare the errors of the fitting of the MTP with 100 basis functions using five different strategies, namely fitting on the entire database (passive learning), selecting 100 random configurations, and three AL approaches. The result for the random selection was averaged over 16 independent samples.

As can be seen from Table 2, all AL methods yield marginal increase in the RMS error as compared to passive learning and decrease in the maximal error. Also, they produce smaller errors than the random selection query strategy. This indicates the efficiency of the AL methods.

Validation test

We next show that applying AL to the fitting of potentials on a fixed database somewhat increases their transferability. To that end, we generated a validation database from an AIMD trajectory at $T = 450$ K (which is close to the melting point of Li) and used it to test the accuracy of the potentials. This database contains configurations significantly different from the training database, and therefore offers a nontrivial transferability test. As can be seen from Table 3, all AL potentials show better accuracy than non-AL potentials on this test.

Table 3: Accuracy validation for different MTPs.

Query strategy	energy error (meV/atom)		force error (eV/Å)		stress error (GPa)	
	RMS	max	RMS	max	RMS	max
passive	0.28	1.5	0.022	0.98	0.071	0.17
random	0.30	1.4	0.023	1.24	0.072	0.21
QS ₁	0.26	1.4	0.021	0.62	0.071	0.17
QS ₂	0.28	1.5	0.022	0.75	0.072	0.16
QS ₃	0.27	1.2	0.022	0.56	0.076	0.17

Robustness test

When an ML potential is used outside its training domain, the results may be unphysical due to large extrapolation errors. The worst-case scenario is that the MD trajectory is stuck at some unphysical domain (for example, when interatomic distances become too short) or even fail due to instability. The purpose of the next test is to explore whether AL, when applied to a fixed database as in the previous test, can produce a more robust interatomic potential.

We use the potentials from the previous test fitted on MD trajectories at $T = 300$ K and use it in MD at $T = 300$ K and $T = 450$ K. We measure the simulation time until the minimal interatomic distance becomes less than 1.5Å (half the Li lattice constant)—sufficiently small to conclude with certainty that the trajectory went into an unphysical region. We call this simulation time the *failure time*. We performed 100 MD runs and calculated the expected failure time for different MTPs. These results are presented in Table 4. As one can see, the actively learned MTPs are more stable as compared to the passively learned ones. Interestingly the neighborhood-based active learning, QS₃, shows by far the best results then the other two active learning approaches. We speculate that this is because the failure most likely happens locally, when two atoms come too close, and QS₃ naturally selects such configurations for training.

Table 4: Average simulation time until some bond is compressed beyond 1.5\AA , which we call the failure time.

Query strategy	# X_{TS}	failure time (ns)	
		$T = 300\text{ K}$	$T = 450\text{ K}$
passive	24000	0.15	0.06
QS ₁	100	0.32	0.14
QS ₂	84	0.63	0.31
QS ₃	92	4.22	3.64

A posteriori error control test

In order to study the correlation between the MLIP errors and the extrapolation grade, we have computed both of them at each time step of MD at $T = 300\text{ K}$. The force errors versus the extrapolation grade are plotted in Figure 2. A good correlation between the two can be observed—this indicates that in practice an extrapolation grade can predict the correct order of magnitude of the error a potential makes on a given configuration without performing a QM calculation.

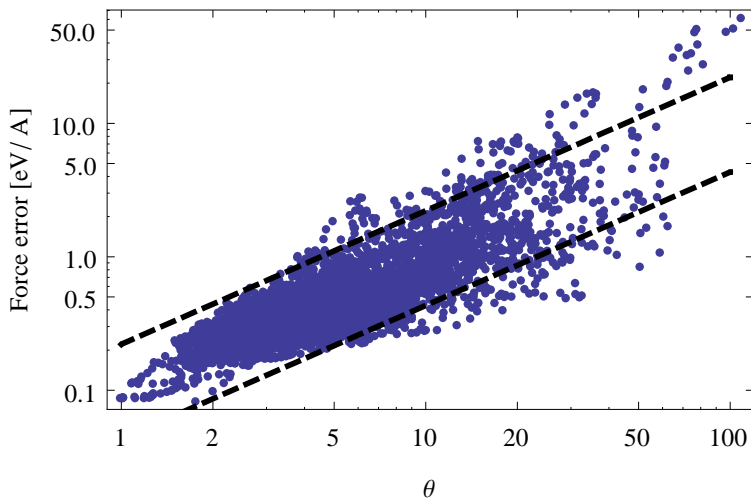
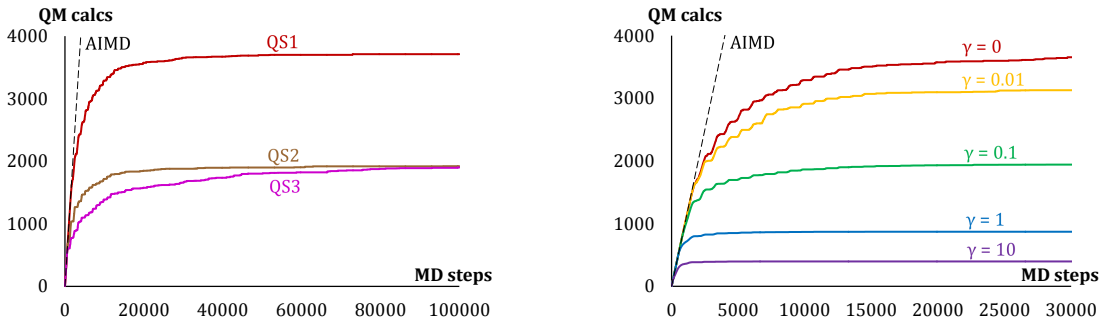


Figure 2: Correlation between the extrapolation grade $\theta(x)$ and the force error $\Delta f(x) = \left(\frac{1}{N} \sum_{i=1}^N |f_i(x) - f_i^q(x)|^2\right)^{1/2}$. For 95% of configurations the RMS force error is between $0.04\theta\text{ eV/\AA}$ and $0.22\theta\text{ eV/\AA}$ (dashed lines)—this indicates a good correlation between the error and the extrapolation grade.

4.2 Learning on the Fly

Next we test our AL strategies in a realistic setting of a learning-on-the-fly MD. We run MD trajectories at $T = 300\text{ K}$ for 100 ps, training MTP on the fly. Graphs in Figure 3a show the amount of QM calculations as a function of the simulation time. One can see that all query strategies require many QM calculations during an initial phase (1–5ps) and then gradually

move to the regime when QM calculations are required only rarely. QS_1 requires about twice more QM calculations as compared to QS_2 and QS_3 .



(a) Comparison of the query strategies.

(b) QS_1 with different thresholds γ (first 30 ps).

Figure 3: Amount of QM calculations as a function of the MD time step.

The amount of the QM calculations drops significantly as γ increases (with $\gamma = 1$ about four times less QM calculations are required as compared to $\gamma = 0$). On the other hand, as seen from Table 5, the errors essentially do not increase up to $\gamma = 1$ and show slight increase at $\gamma = 10$ (for $\gamma > 0$ only the errors of QS_1 are tabulated, however, the behavior of QS_2 and QS_3 with increasing γ is essentially the same). This indicates that one can easily tune the efficiency-versus-accuracy performance of an AL scheme by adjusting γ .

Table 5: Accuracy validation for different MTPs.

Query strategy	γ	#QM calcs	energy error (meV/atom)		force error (eV/Å)		stress error (GPa)	
			RMS	max	RMS	max	RMS	max
QS_1	0	3712	0.18	0.56	0.015	0.13	0.057	0.19
QS_1	0.1	1958	0.18	0.71	0.016	0.19	0.056	0.20
QS_1	1	873	0.19	0.76	0.016	0.13	0.055	0.22
QS_1	10	397	0.27	0.83	0.016	0.31	0.050	0.27
QS_2	0	1921	0.22	0.75	0.016	0.09	0.056	0.20
QS_3	0	1900	0.19	0.85	0.015	0.12	0.057	0.23

5 Discussion

Our results suggest that the proposed learning-on-the-fly algorithms do not reduce the accuracy of MLIPs while always keeping the MD trajectory within the physical region. It should also be emphasized that the AL algorithm introduces a computational overhead that, at least in our test examples, was less expensive than calculating the energy, forces and stresses. The

overhead of re-training our potential was also small compared to the time of calculating the energy, forces and stresses.

Our AL algorithms can work on configurations with varying number of atoms. This may be important in many applications, including computational structure prediction [17] where the sought configurations may be of unknown size.

The choice of the D-optimality criterion, which our AL algorithms are based on, was motivated by reducing uncertainty in the potential parameters. However, there is also another interpretation. For example, the elements of the matrix A in QS_1 , $b_j(x^{(k)})$, can be considered as descriptors of the configuration $x^{(k)}$, each configuration is characterized by an m -dimensional descriptor vector. In this sense the D-optimality criterion maximizes the volume of the simplex in \mathbb{R}^m formed by m descriptor vectors. In the same way $B_{\alpha_j}(\mathbf{r}_i^{(k)})$, which are the elements of matrix A in QS_3 , can be considered as the descriptors of a neighborhood of atom i of k -th configuration. Therefore, QS_3 “catches” configurations in X_{US} with the most different atomic neighborhoods in the sense of the D-optimality criterion. This property of QS_3 can be used in a learning-on-the-fly MD with million or more atoms where training has to be done on local environments completed to small configurations.

The query strategies QS_1 – QS_3 differ from each other by a number of properties and no single one is better than the other ones. QS_1 is the most computationally efficient and yields a slightly more accurate MLIP. However, it needs about twice more QM calculations than QS_2 and QS_3 while learning on the fly. QS_2 is the most expensive scheme but has the lowest maximal force error. QS_3 creates a significantly more robust potential offline, presumably because it is designed to choose the most different neighborhoods.

6 Conclusion

Machine learning interatomic potentials offer a promising way of combining the accuracy of quantum mechanics and the computational efficiency of the empirical interatomic potentials. However, the weak point of the machine learning interatomic potentials is reliability—the more general and accurate they are required to be, the harder it is to generate offline the training dataset that ensures no extrapolation at the online evaluation stage. In the present work we have shown that this problem can be solved by applying active learning to the fitting of the machine learning interatomic potentials.

We have proposed a new active learning scheme based on the D-optimality criterion and have shown empirically that it yields an accurate, computationally efficient, and reliable interatomic interaction model. In particular, using active learning in the learning-on-the-fly scenario fully resolves the transferability problem—active learning detects when extrapolation is attempted and re-trains the potential on those configurations. In the case when learning on the fly cannot be performed, the proposed active learning techniques allow one to control the degree of extrapolation. In addition, active learning applied offline can improve robustness of the potentials and reduce the training set size, while keeping the accuracy at the same level.

7 Acknowledgments

The authors thank Prof. Ivan Oseledets for useful discussions of application of the D-optimality criterion in active learning. This work was supported by the Skoltech NGP Program No. 2016-7/NGP (a Skoltech-MIT joint project). A part of the work was done by A.S. during the Fall 2016 long program at the Institute of Pure and Applied Mathematics, UCLA.

A Appendix A: Maxvol algorithm

The query strategies QS₂ and QS₃ require finding the $m \times m$ submatrix \mathbf{A} with maximal $|\det \mathbf{A}|$ (or, in other words, with the maximal volume) in an $k \times m$ matrix \mathbf{B} . This is done by the maxvol algorithm [22]. This algorithm is based on greedy selection of rows from \mathbf{B} . Each iteration of this algorithm has $O(mk)$ complexity. The algorithm is as follows.

1. Start with an initial (e.g., randomly chosen) $m \times m$ submatrix \mathbf{A} of \mathbf{B} and calculate $\mathbf{C} = \mathbf{B}\mathbf{A}^{-1}$.
2. Find the maximal by absolute value element \mathbf{C}_{ij} in this matrix.
3. If $|\mathbf{C}_{ij}| > 1 + \gamma$ then:
 - 3.1 swap the i -th row of \mathbf{A} with the j -th row of \mathbf{B} ,
 - 3.2 update $\mathbf{C} = \mathbf{B}\mathbf{A}^{-1}$ using the Sherman-Morrison [33] rank-one update,
 - 3.3 go to step 2.

The smaller the threshold parameter $\gamma > 0$ is, the larger $|\det \mathbf{A}|$ will be, at the cost of making more iterations.

References

- [1] E. Artacho, D. Sánchez-Portal, P. Ordejón, A. Garcia, and J. M. Soler. Linear-scaling ab-initio calculations for large and complex systems. *arXiv preprint cond-mat/9904159*, 1999.
- [2] N. Artrith and A. M. Kolpak. Grand canonical molecular dynamics simulations of cu–au nanoalloys in thermal equilibrium using reactive ann potentials. *Computational Materials Science*, 110:20–28, 2015.
- [3] A. P. Bartók, M. J. Gillan, F. R. Manby, and G. Csányi. Machine-learning approach for one-and two-body corrections to density functional theory: Applications to molecular and condensed water. *Physical Review B*, 88(5):054104, 2013.
- [4] A. P. Bartók, R. Kondor, and G. Csányi. On representing chemical environments. *Physical Review B*, 87(18):184115, 2013.

- [5] A. P. Bartók, M. C. Payne, R. Kondor, and G. Csányi. Gaussian approximation potentials: The accuracy of quantum mechanics, without the electrons. *Phys. Rev. Lett.*, 104:136403, Apr 2010.
- [6] J. Behler. Atom-centered symmetry functions for constructing high-dimensional neural network potentials. *The Journal of chemical physics*, 134(7):074106, 2011.
- [7] J. Behler. Neural network potential-energy surfaces in chemistry: a tool for large-scale simulations. *Physical Chemistry Chemical Physics*, 13(40):17930–17955, 2011.
- [8] J. Behler. Representing potential energy surfaces by high-dimensional neural network potentials. *Journal of Physics: Condensed Matter*, 26(18):183001, 2014.
- [9] J. Behler and M. Parrinello. Generalized neural-network representation of high-dimensional potential-energy surfaces. *Physical review letters*, 98(14):146401, 2007.
- [10] J. R. Boes, M. C. Groenenboom, J. A. Keith, and J. R. Kitchin. Neural network and ReaxFF comparison for Au properties. *International Journal of Quantum Chemistry*, 116(13):979–987, 2016.
- [11] V. Botu, R. Batra, J. Chapman, and R. Ramprasad. Machine learning force fields: Construction, validation, and outlook. *arXiv preprint arXiv:1610.02098*, 2016.
- [12] V. Botu and R. Ramprasad. Adaptive machine learning framework to accelerate ab initio molecular dynamics. *International Journal of Quantum Chemistry*, 115(16):1074–1083, 2015.
- [13] V. Botu and R. Ramprasad. Learning scheme to predict atomic forces and accelerate materials simulations. *Physical Review B*, 92(9):094306, 2015.
- [14] D. R. Bowler and T. Miyazaki. Calculations for millions of atoms with density functional theory: linear scaling shows its potential. *Journal of Physics: Condensed Matter*, 22(7):074207, 2010.
- [15] K. Burke et al. The ABC of DFT. *Department of Chemistry, University of California*, 2007.
- [16] V. L. Deringer and G. Csányi. Machine-learning based interatomic potential for amorphous carbon. *arXiv preprint arXiv:1611.03277*, 2016.
- [17] P. E. Dolgirev, I. A. Kruglov, and A. R. Oganov. Machine learning scheme for fast extraction of chemically interpretable interatomic potentials. *AIP Advances*, 6(8):085318, 2016.
- [18] F. Faber, A. Lindmaa, O. A. von Lilienfeld, and R. Armiento. Crystal structure representations for machine learning models of formation energies. *International Journal of Quantum Chemistry*, 115(16):1094–1101, 2015.
- [19] M. Finnis. *Interatomic forces in condensed matter*, volume 1. OUP Oxford, 2003.

- [20] S. L. Frederiksen, K. W. Jacobsen, K. S. Brown, and J. P. Sethna. Bayesian ensemble approach to error estimation of interatomic potentials. *Physical review letters*, 93(16):165501, 2004.
- [21] M. Gastegger and P. Marquetand. High-dimensional neural network potentials for organic reactions and an improved training algorithm. *Journal of chemical theory and computation*, 11(5):2187–2198, 2015.
- [22] S. Goreinov, I. Oseledets, D. Savostyanov, E. Tyrtysnikov, and N. Zamarashkin. How to find a good submatrix. In *Matrix Methods: Theory, Algorithms, Applications*, pages 247–256. World Scientific, 2010.
- [23] G. Kresse and J. Furthmüller. Efficiency of ab-initio total energy calculations for metals and semiconductors using a plane-wave basis set. *Computational Materials Science*, 6(1):15–50, 1996.
- [24] G. Kresse and J. Furthmüller. Efficient iterative schemes for ab initio total-energy calculations using a plane-wave basis set. *Physical review B*, 54(16):11169, 1996.
- [25] G. Kresse and J. Hafner. Ab initio molecular dynamics for liquid metals. *Physical Review B*, 47(1):558, 1993.
- [26] Z. Li, J. R. Kermode, and A. De Vita. Molecular dynamics with on-the-fly machine learning of quantum-mechanical forces. *Phys. Rev. Lett.*, 114:096405, Mar 2015.
- [27] S. Manzhos, R. Dawes, and T. Carrington. Neural network-based approaches for building high dimensional and quantum dynamics-friendly potential energy surfaces. *International Journal of Quantum Chemistry*, 115(16):1012–1020, 2015.
- [28] T. Mueller, A. G. Kusne, and R. Ramprasad. Machine learning in materials science: Recent progress and emerging applications. *Rev. Comput. Chem*, 2015.
- [29] S. K. Natarajan, T. Morawietz, and J. Behler. Representing the potential-energy surface of protonated water clusters by high-dimensional neural network potentials. *Physical Chemistry Chemical Physics*, 17(13):8356–8371, 2015.
- [30] M. Rupp, A. Tkatchenko, K.-R. Müller, and O. A. Von Lilienfeld. Fast and accurate modeling of molecular atomization energies with machine learning. *Physical review letters*, 108(5):058301, 2012.
- [31] B. Settles. Active learning literature survey. Computer Sciences Technical Report 1648, University of Wisconsin–Madison, 2009.
- [32] A. Shapeev. Moment tensor potentials: a class of systematically improvable interatomic potentials. *Multiscale Model. Simul.*, 14(3):1153–1173, 2016.
- [33] J. Sherman and W. J. Morrison. Adjustment of an inverse matrix corresponding to a change in one element of a given matrix. *The Annals of Mathematical Statistics*, 21(1):124–127, 1950.

- [34] C.-K. Skylaris, P. D. Haynes, A. A. Mostofi, and M. C. Payne. Introducing ONETEP: Linear-scaling density functional simulations on parallel computers. *The Journal of chemical physics*, 122(8):084119, 2005.
- [35] J. S. Smith, O. Isayev, and A. E. Roitberg. Ani-1: An extensible neural network potential with dft accuracy at force field computational cost. *arXiv preprint arXiv:1610.08935*, 2016.
- [36] J. C. Snyder, M. Rupp, K. Hansen, K.-R. Müller, and K. Burke. Finding density functionals with machine learning. *Physical review letters*, 108(25):253002, 2012.
- [37] W. J. Szlachta, A. P. Bartók, and G. Csányi. Accuracy and transferability of Gaussian approximation potential models for tungsten. *Physical Review B*, 90(10):104108, 2014.
- [38] A. Thompson, L. Swiler, C. Trott, S. Foiles, and G. Tucker. Spectral neighbor analysis method for automated generation of quantum-accurate interatomic potentials. *Journal of Computational Physics*, 285:316 – 330, 2015.
- [39] I. Torrens. *Interatomic potentials*. Elsevier, 2012.